33rd Annual International Conference of the IEEE EMBS
Boston, Massachusetts USA, August 30 - September 3, 2011

A MOM/FEM-based coil sensitivity mapping method for high-field parallel MRI

Jin Jin[1], Feng Liu[1], Yu Li[1], Ewald Weber[1], Wenlong Xu[2] and Stuart Crozier[1], *Member, IEEE*

***Abstract*— In this study, an electromagnetics-based inverse sensitivity mapping method is introduced for applications in high field MRI. Instead of using simplistic numerical approximations, the sensitivity of the radio-frequency coil was determined through a field approach by using iterative optimization. The current study is an extension to previous studies on the inverse method, which has restricted itself to low-field applications due to the use of the Biot-Savart integration to account for the H field calculations. In the current study, full-wave solutions to the Maxwell's equations based MOM/FEM hybrid algorithm were employed to provide H field evaluation. It is demonstrated that the proposed method is able to produce high-fidelity sensitivity estimation which result in images with significantly less artefact power.**

I. Introduction

THIS paper extends our previous studies on the electromagnetics-based inverse method of sensitivity mapping [1, 2] and eliminates the restriction to low-field applications, so that the method is generic to low-field as well as high-field image reconstructions in the parallel magnetic resonance imaging (pMRI). To reconstruct images with high fidelity, accurate sensitivity mapping is crucial for image-domain methods which are often the preferred methods for pMRI.

The preference of the image-domain methods becomes clear when the underlying mechanisms of the K-space methods and image-domain methods are compared. These algorithms share the same encoding mechanism [3], Fourier encoding owing to the gradients and sensitivity encoding owing to the receptivity profiles of each element in the array. As a result, they are often viewed as different approaches to solving the same inverse problem [3, 4]. However, different algorithms dictate different procedures. The K-space approaches estimate the linear combination coefficients from the auto-calibration signal (ACS) [5, 6] and repopulate the missing lines by applying these coefficients to the acquired lines. Consequently, K-space approaches generally yield only approximations to the solution of the linear equations. Image-domain approaches [7, 8], on the other hand, formulate the Fourier and sensitivity encoding as well as acquired data into a single set of linear simultaneous equations. The image, resolved by direct inversion, is the maximum signal-to-noise ratio (SNR) solution [3]. The direct inversion can be replaced by iterative approaches since it can be prohibitively demanding in computational power [8]. Additionally, regularization terms can be incorporated into iterative approaches to achieve noise mitigation [9, 10].

However, optimal image reconstructions are often hindered by suboptimal coil array geometries and inaccurate sensitivity estimations. Although research on optimising array arrangements is on-going, little has been done to improve the accuracy of sensitivity estimation. Instead of refining raw sensitivity maps by means of image/signal processing [7, 11, 12], we propose making use of the reciprocity theory [13, 14], which allows the evaluation of the receiving sensitivity (B_1^-) from the transmitting field (B_1^+) of a certain coil element. To do this, a low-resolution raw sensitivity B_1^- is first examined; the equivalent B_1^+ field is then used to inversely determine the coil-phantom geometry through optimization. Full-wave solutions to Maxwell's equations will be employed to evaluate the B_1^+ field, as opposed to the use of Biot-Savart integration (Ampere's Law with quasi-static limits). To test if the proposed method is suitable for both low-field and high-field applications, as is expected when the quasi-static limits are lifted, we will analyse two cases. The first case tests the procedure of the proposed method in a simple coil setup, whereas the second case evaluates the new method in a 6-element overlapping array at 7T.

II. Methods

The theory of reciprocity [13, 14] allows the evaluation of coil reception sensitivity from transmitting fields. To evaluate the transmit B_1^+ profile, a series of operations have to be followed. First, the coil-phantom geometry is modelled according to the physical setup. This geometry is then adjusted to allow variations in fabrication by minimizing the measured raw sensitivity and the calculated sensitivity through an iterative optimization. Finally, while the geometry more closely resembles the real-world physical setup, the calculated sensitivity profile approaches the ideal noise-free coil sensitivity. In low field cases, as demonstrated in [2], the evaluation of transmit B_1^+ is reduced to Biot-Savart integration for the calculation of the magnetic field. In cases of higher static magnetic field, the

Manuscript received March 25, 2011.

[1]J. Jin, Y. Li, F. Liu, E. Weber and S. Crozier are with the School of Information Technology and Electrical Engineering, the University of Queensland, Brisbane, Queensland 4072, Australia.

[2]W, Xu is with the Department of Biomedical Engineering, China Jiliang University, China

Emails: jinjin@itee.uq.edu.au (J. Jin); yuli@itee.uq.edu.au (Y. Li); feng@itee.uq.edu.au (F. Liu); ewald@itee.uq.edu.au (E. Weber) and stuart@itee.uq.edu.au (S. Crozier).

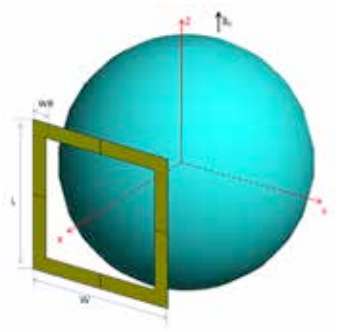

Fig 1 modelling of single-loop RF coil at 300MHz

Biot-Savart integration is no longer an accurate estimation due to the shortened electrical wavelength and the wave behaviour within the scanned object [15]. In this study, a hybrid MOM/FEM method is used to provide a numerical full-wave solution for the high-field cases [15, 16]. The optimization process is controlled by a program written in Matlab (Mathworks, Natick, MA). The cost function invokes FEKO (EMSS, SA) to calculate the transverse magnetic field; and returns the differences between calculated and measured sensitivity. The differences were weighted by a smoothed raw sensitivity, giving stronger bias towards the area in close vicinity to the RF coil. An implementation of the Nelder-Mean simplex optimization algorithm [17] is used to minimize this cost function. As simplex algorithms are generally unconstrained optimization, extra terms are added to the cost function to ensure the optimized values are within the respective lower and upper bounds. In the following paragraphs, the proposed method will be presented in two case studies.

A. A single-loop radio-frequency (RF) coil

In this case study, the proposed method was demonstrated in the simplest scenario. As shown Fig-1, a single-loop 300MHz RF coil is modelled in FEKO. The coil has dimensions as follows: length L=80 mm, width W=80 mm and width of strip WB=8 mm. The coil is located 10 mm away from the phantom along the x-axis. It is loaded with a spherical phantom with radius R=62.5 mm; relative permittivity ε_r=50; and conductivity σ=0.6 S/m. After tuning and matching, the magnetic field at plane z=0 was calculated (Fig-2a).

To obtain the raw sensitivity profile, the following steps were employed. Firstly, a sensitivity-weighted coil image was produced by pixel-wise multiplication between the noise-free sensitivity from FEKO and the original image. Secondly, a controlled amount of noise was added to the real and imaginary channel of the image in K-space to simulate the noisy coil images. Thirdly, noise was similarly introduced into the uniform reference image. Finally, the quotient of the noisy coil image by the noisy reference image yields the raw sensitivity (Fig-2b).

This raw sensitivity can be directly fed to the optimization procedure. However, it was found that the optimization converged more rapidly when a smoother sensitivity profile was used. Therefore, localized polynomial fitting was performed before passing sensitivity estimation to optimization. The parameters of polynomial fittings that yield the best reconstruction quality were determined empirically. Fig-3 shows the root mean square deviation (RMSD) between the reconstructed image and the original image when polynomial fitting was applied to refine the sensitivity. It can be seen that higher order fitting requires a bigger window to generate reliable fittings. In most cases, second order fittings give the best reconstruction, which is expected, given the slow-changing nature of the profile.

A binary mask was applied to the fitted profile (Fig-2c) to avoid unnecessary calculations during the reconstruction [8]. This fitted profile was then used as a target profile in the optimization. The stopping criteria were set to be 0.01 for both the tolerance of function value and the tolerance of optimizing variables. The inverse method resulted in an optimized full field-of-view (FOV) sensitivity (Fig-2d). The fitted profile and inversely determined profile were used in a simulated 4-channel parallel reconstruction, as shown in Fig-2e and 2f respectively. Estimated sensitivity was rotated 90°, 180° and 270° to generate sensitivities for the other elements in the array.

B. 6-element 7T knee coil array

A 6-element 7T overlapping array was adopted in this case study to demonstrate the feasibility of using the proposed method to inversely determine the sensitivity profile of any element in an array. This 6-element overlapping array was modelled in FEKO (Fig-4) with element height H=100 mm, open angle OA=76.85°, width of strip WB=8 mm and distance to phantom D=10 mm. The spherical phantom has the same geometrical and dielectric properties as in the previous case.

Similar to the single-loop RF-coil study, a series of operations were performed to simulate sensitivity mapping and image reconstruction for the 6-element 7T knee coil array. Shown in Fig-5 are noise-free sensitivity profiles (a) obtained from FEKO modelling and simulations. A noisy raw sensitivity (b) was then calculated. Two-dimensional

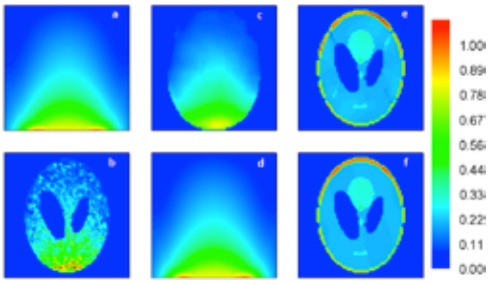

Fig 2 sensitivity profile and reconstructed images for single-loop RF coil at 300MHz. a – noise-free sensitivity derived from FEKO simulation; b – simulated raw sensitivity profile (with mask); c – refined sensitivity by means of localized two-dimensional polynomial fitting; d - sensitivity profile obtained through the proposed method; e – reconstructed image using sensitivity data from c; and f - reconstructed image using sensitivity data from d.

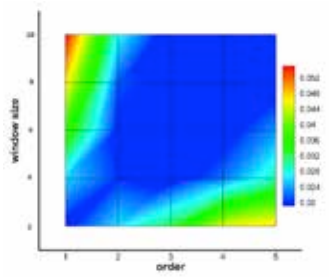

Fig 3 error of image reconstruction versus polynomial fitting order and window size used to refine sensitivity profile

polynomial fitting was performed to refine the raw profile (c). The proposed inverse method was then carried out (d). Images (e) and (f) were afterwards reconstructed using profile (c) and profile (d), respectively.

III. Results

To evaluate its performance, the proposed method is compared to the traditional method in terms of the accuracy of the estimated sensitivity profile and the image quality when the estimated sensitivity profiles were used in image reconstruction. A specific case with 30dB SNR [2] is displayed in Fig-6. (a) and (e) show the sensitivity profiles estimated using the polynomial fitting and the inverse method respectively. The difference between estimated profiles and the original noise-free profile are shown in (b) and (f). The sensitivity profile derived from the inverse method shows significant improvement over the polynomial fitting in terms of the magnitude and the distribution of the error. Images (c) and (g) were reconstructed [8] using profile (b) and (f). Reconstruction artefact is clearly visible in (c), while artefacts can hardly be seen in (g). It becomes clear that the increased accuracy in sensitivity estimation results in superior image reconstruction, when images (d) and (h) – the difference between reconstructed images and the original image – are examined side by side.

For the single-rung RF coil study, the root mean square deviation (RMSD) was calculated to quantify the error of sensitivity estimation, whereas artefact power (AP) was used to measure the quality of image reconstruction. The RMSD of the estimated sensitivity by using the polynomial fitting and the inverse method are shown on the top of Fig-7. The inverse method has definite advantages over the traditional method in sensitivity estimation for all SNR levels. This in

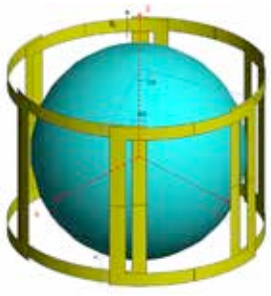

Fig 4 modelling of 7T 6-element overlapping knee coil

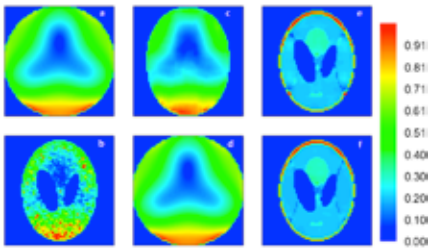

Fig 5 sensitivity profile and reconstructed images for 6-element knee coil at 300MHz. a – noise-free sensitivity derived from FEKO simulation; b – simulated raw sensitivity profile (with mask); c – refined sensitivity by means of localized two-dimensional polynomial fitting; d – sensitivity profile obtained through the proposed method; e – reconstructed image using sensitivity data from c; and f - reconstructed image using sensitivitv data from d.

turn leads to superior image construction with the AP of images at least an order of magnitude less than that of the traditional method, as shown on the bottom of Fig-7. Similar results for the 6-element 7T knee coil array are shown in Fig-8, in which the proposed method generated more accurate sensitivity compared to the traditional method, leading to significantly less artefact power in the reconstructed images.

IV. Discussion and Conclusion

The concept of obtaining the sensitivity profile of a RF coil by field approaches rather than numerical approximations has been proposed [1, 2]. In the current study, the inverse method was extended to map the RF array

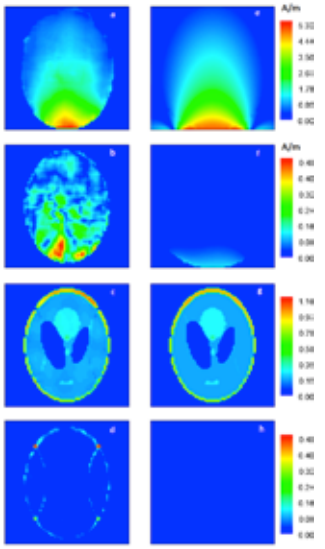

Fig 4 the comparisons of the traditional polynomial fitting and the proposed inverse method. The first and the second column depict the results using the two-dimensional polynomial fitting and the inverse method, respectively. a, g – estimation of sensitivity profiles; b, f – difference between the estimated and the true sensitivity; c, g – reconstructed images using b and f; d, h – difference between the reconstructed images and the original image.

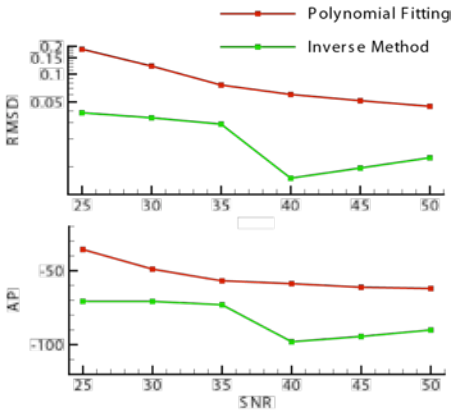

Fig 5 results of single-loop case study. Top: RMSD of the estimated sensitivity profile by using polynomial fitting (red) and the proposed method (green). Bottom: AP of the reconstructed images by using polynomial fitting (red) and the proposed method (green).

sensitivity at high fields. A single-loop loaded RF coil and a 6-element overlapping knee coil array were used to demonstrate the feasibility of the method at 7T. A MOM/FEM hybrid method was adopted to provide efficient full-wave solutions to Maxwell's equations. A simplex optimization algorithm was then implemented to search for the B_1 profile that has the least discrepancies with the raw sensitivity. It was demonstrated that the proposed method successfully estimated the coil sensitivity with lower noise amplitude, and that the reconstructed images presented less artefact power compared to the traditional method.

The proposed method is not restricted to either dynamic or static mapping. Low resolution raw sensitivity profiles were used in the proposed method, since the raw profiles were merely used to inversely determine the geometrical variables of the RF coils, which can then generate high resolution sensitivity by forward calculation. The alleviated resolution requirement on raw sensitivity estimations relaxes reference scan time considerably without sacrificing the quality of sensitivity estimation. Future studies will focus on applying the proposed method in imaging studies.

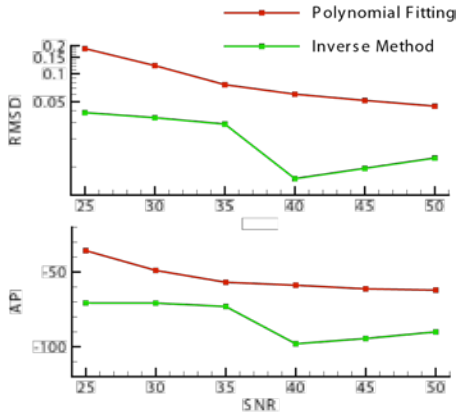

Fig 6 results of 6-element array at 7T. Top: RMSD of the estimated sensitivity profile by using polynomial fitting (red) and the proposed method (green). Bottom: AP of the reconstructed images by using polynomial fitting (red) and the proposed method (green).

ACKNOWLEDGEMENT

This work was supported by the Australia research council and the Science and Technology Department of Zhejiang province, China, project ID- 2010C14010.

REFERENCES

[1] J. Jin, *et al.*, "Maxwell's equation tailored reverse method of sensitivity mapping for parallel MRI," presented at the ISMRM-ESMRMB Joint Annual Meeting 2010, Stockholm, Sweden, 2010.

[2] J. Jin, *et al.*, "An electromagnetic reverse method of coil sensitivity mapping for parallel MRI - Theoretical framework," *Journal of Magnetic Resonance,* vol. 207, pp. 59-68, 2010.

[3] K. P. Pruessmann, "Encoding and reconstruction in parallel MRI," *Nmr in Biomedicine,* vol. 19, pp. 288-299, 2006.

[4] D. K. Sodickson and C. A. McKenzie, "A generalized approach to parallel magnetic resonance imaging," *Medical Physics,* vol. 28, pp. 1629-1643, Aug 2001.

[5] D. K. Sodickson and W. J. Manning, "Simultaneous acquisition of spatial harmonics (SMASH): Fast imaging with radiofrequency coil arrays," *Magnetic Resonance in Medicine,* vol. 38, pp. 591-603, 1997.

[6] M. A. Griswold, *et al.*, "Generalized Autocalibrating Partially Parallel Acquisitions (GRAPPA)," *Magnetic Resonance in Medicine,* vol. 47, pp. 1202-1210, Jun 2002.

[7] K. P. Pruessmann, *et al.*, "SENSE: Sensitivity encoding for fast MRI," *Magnetic Resonance in Medicine,* vol. 42, pp. 952-962, 1999.

[8] K. P. Pruessmann, *et al.*, "Advances in sensitivity encoding with arbitrary k-space trajectories," *Magnetic Resonance in Medicine,* vol. 46, pp. 638-651, Oct 2001.

[9] F. H. Lin, *et al.*, "Parallel imaging reconstruction using automatic regularization," *Magnetic Resonance in Medicine,* vol. 51, pp. 559-567, Mar 2004.

[10] J. Sánchez-González, *et al.*, "Minimum-norm reconstruction for sensitivity-encoded magnetic resonance spectroscopic imaging," *Magnetic Resonance in Medicine,* vol. 55, pp. 287-295, 2006.

[11] C. A. McKenzie, *et al.*, "Self-calibrating parallel imaging with automatic coil sensitivity extraction," *Magnetic Resonance in Medicine,* vol. 47, pp. 529-538, Mar 2002.

[12] F. H. Lin, *et al.*, "A Wavelet-based Approximation of Surface Coil Sensitivity Profiles for Correction of Image Intensity Inhomogeneity and Parallel Imaging Reconstruction," *Human Brain Mapping,* vol. 19, pp. 96-111, Jun 2003.

[13] D. I. Hoult, "The principle of reciprocity in signal strength calculations - A mathematical guide," *Concepts in Magnetic Resonance,* vol. 12, pp. 173-187, 2000.

[14] T. S. Ibrahim, "Analytical approach to the MR signal," *Magnetic Resonance in Medicine,* vol. 54, pp. 677-682, Sep 2005.

[15] F. Liu, *et al.*, "Numerical modeling of 11.1T MRI of a human head using a MoM/FDTD method," *Concepts in Magnetic Resonance Part B: Magnetic Resonance Engineering,* vol. 24B, pp. 28-38, 2005.

[16] B. K. Li, *et al.*, "High-Field Magnetic Resonance Imaging With Reduced Field/Tissue RF Artefacts—A Modeling Study Using Hybrid MoM/FEM and FDTD Technique," *Electromagnetic Compatibility, IEEE Transactions on,* vol. 48, pp. 628-633, 2006.

[17] C. L. Jeffrey, *et al.*, "Convergence Properties of the Nelder-Mead Simplex Method in Low Dimensions," ed, 1998.